Proc. Natl. Acad. Sci. USA
Vol. 92, pp. 8710–8714, September 1995
Neurobiology

Identification and localization of huntingtin in brain and human lymphoblastoid cell lines with anti-fusion protein antibodies

CLAIRE-ANNE GUTEKUNST*, ALLAN I. LEVEY*, CRAIG J. HEILMAN*, WILLIAM L. WHALEY†, HONG YI*, NORMAN R. NASH*, HOWARD D. REES*, JOHN J. MADDEN†, AND STEVEN M. HERSCH*‡

Departments of *Neurology and †Psychiatry, Emory University School of Medicine, Atlanta, GA 30322

Communicated by Patricia S. Goldman-Rakic, Yale University, New Haven, CT, June 9, 1995

ABSTRACT **The Huntington disease (HD) phenotype is associated with expansion of a trinucleotide repeat in the *IT15* gene, which is predicted to encode a 348-kDa protein named huntingtin. We used polyclonal and monoclonal anti-fusion protein antibodies to identify native huntingtin in rat, monkey, and human. Western blots revealed a protein with the expected molecular weight which is present in the soluble fraction of rat and monkey brain tissues and lymphoblastoid cell lines from control cases. In lymphoblastoid cell lines from juvenile-onset heterozygote HD cases, both normal and mutant huntingtin are expressed, and increasing repeat expansion leads to lower levels of the mutant protein. Immunocytochemistry indicates that huntingtin is located in neurons throughout the brain, with the highest levels evident in larger neurons. In the human striatum, huntingtin is enriched in a patch-like distribution, potentially corresponding to the first areas affected in HD. Subcellular localization of huntingtin is consistent with a cytosolic protein primarily found in somatodendritic regions. Huntingtin appears to particularly associate with microtubules, although some is also associated with synaptic vesicles. On the basis of the localization of huntingtin in association with microtubules, we speculate that the mutation impairs the cytoskeletal anchoring or transport of mitochondria, vesicles, or other organelles or molecules.**

Huntington disease (HD) is an inherited neurodegenerative disorder characterized by progressive motor, psychiatric, and cognitive disturbances. The neuropathology of HD includes selective loss of neurons that is most severe in the caudate and putamen but also affects other brain regions. It has been hypothesized that neuronal death in HD is due to a metabolic defect that leads to excitotoxicity (1, 2). The genetic mutation, however, has not yet been directly linked to neuronal metabolism.

HD has been associated with the abnormal expansion of a polymorphic trinucleotide (CAG) repeat sequence occurring in the coding region of a gene (*IT15*) located on chromosome 4 (3). In HD, the length of this repeat is substantially increased, ranging from 40 to over 100 copies (3–5). Juvenile-onset HD cases are associated with the highest numbers of repeats (3, 6). The *IT15* gene encodes a large unknown protein (≈343 kDa) that has been termed "huntingtin" (3). Its mRNA is normally distributed in diverse tissues in human and rat (3, 7) and is expressed predominantly in neurons in brain (7, 8). In HD heterozygotes, both normal and mutant mRNA are present, suggesting that the trinucleotide expansion does not prevent transcription (9). Thus, the pathophysiology of HD likely depends on the effect of the mutant allele at the protein level. Understanding huntingtin is therefore crucial for determining how the genetic mutation could be linked to the pathophysiology of HD and for developing treatments based on the molecular defect. We have developed polyclonal and monoclonal antibodies specific to huntingtin to enable its identification. We have identified native huntingtin in rat, monkey, and human tissues and both normal and mutant proteins in lymphoblast cell lines established from HD patients. With light and electron microscopic immunocytochemistry, we have examined the cellular and subcellular localization of huntingtin in brain.

The publication costs of this article were defrayed in part by page charge payment. This article must therefore be hereby marked "*advertisement*" in accordance with 18 U.S.C. §1734 solely to indicate this fact.

MATERIALS AND METHODS

Antibody Production and Characterization. Rabbit polyclonal and rat monoclonal antibodies specific for huntingtin were raised against a recombinant protein derived from a segment of human huntingtin (amino acids 549–679) fused to glutathione *S*-transferase (GST) ($HD_{549-679}$-GST). Fragments of the human huntingtin cDNA were provided as bacteriophage clones by James Gusella (Massachusetts General Hospital) and used as templates for PCR synthesis of the appropriate segment, which was then inserted into pGEX-2T. By using previously described methods (10, 11) the soluble fusion protein was expressed in bacteria, purified, and used as an antigen for the production of affinity-purified rabbit polyclonal antibodies and rat monoclonal antibodies.

Immunoblot Analysis. SDS/PAGE was used to fractionate total protein from either dissected regions of rat and monkey brains or lymphoblasts derived from normal and HD individuals [obtained from the Emory University Huntington's Clinic (Atlanta), the Coriell Institute (Camden, NJ), and the Molecular Neurogenetics Unit at Massachusetts General Hospital (Boston)]. Gels were electroblotted onto Immobilon-P membrane (Millipore) and incubated in affinity-purified polyclonal antibodies (0.5–1 μg/ml) or monoclonal antibodies (diluted 1:250 to 1:500), and specific antigens were visualized by using enhanced chemiluminescence (Amersham) (12). Controls included omission of primary antibodies and preadsorption of antibodies with excess $HD_{549-679}$-GST.

Immunocytochemistry. Light and electron microscopic immunocytochemistry was performed on brain sections from rat (not shown) and from two young adult male rhesus monkeys (*Macacca mulatta*). Each was injected with an overdose of pentobarbital and then perfused intracardially with 0.9% saline followed by 3% (wt/vol) paraformaldehyde/0.1% glutaraldehyde in 0.1 M phosphate buffer. Tissue blocks were sectioned at 40 μm, and immunocytochemistry with 3,3′-diaminobenzidine tetrahydrochloride (DAB; Sigma) as the chromogen was performed as described (13). Polyclonal antibodies were used at a concentration of 1 μg/ml. Monoclonal antibodies were used at a dilution of 1:100. For electron microscopy, selected monkey sections from frontal cortex, putamen, and cerebellum were osmicated and stained over-

Abbreviations: HD, Huntington disease; GST, glutathione *S*-transferase; DAB, 3,3′-diaminobenzidine tetrahydrochloride.

‡To whom reprint requests should be addressed at: Department of Neurology, Emory University School of Medicine, WMB, Suite 6000, P.O. Drawer V, Atlanta, GA 30322.

night in uranyl acetate. Sections were then dehydrated, embedded in Durcupan (Fluka), thin-sectioned, and analyzed by using a JEOL 100C electron microscope. For more precise electron microscopic spatial resolution, we also used immunogold labeling (1.4-nm gold particles; Nanoprobes, Stony Brook, NY) (14) in sections from the same regions. Light microscopic immunocytochemistry was also performed on sections from two human control brains which were from 22- and 83-year-old males with brain weights of 1500 and 1306 g, respectively. Postmortem intervals were 8 and 15 h. Human tissue was fixed by immersion overnight in 4% (wt/vol) paraformaldehyde and cryo-preserved in sucrose/phosphate-buffered saline solution at 4°C. Controls included omission of primary antibodies and preadsorption of antibody with excess $HD_{549-679}$-GST.

RESULTS

Detection of Rat, Monkey, and Human Huntingtin. Polyclonal and monoclonal antibodies reacted strongly with the huntingtin fusion protein antigen and showed no cross-reactivity to bacterial proteins, GST, or other heterologous fusion proteins (data not shown). On immunoblots of rat, monkey, and human tissues, a protein band with an approximate molecular mass of 340 kDa was detected with both polyclonal and monoclonal antibodies (Fig. 1). This molecular mass is consistent with that predicted from the *IT15* open reading frame (3). In lymphoblasts derived from human controls, both antibodies detected a single band. Additional protein bands were detected by the polyclonal antibodies in rat testis (45–50 kDa) and the monoclonal antibodies in monkey brain (130–140 kDa) (Fig. 1). Immunoreactivity for all the bands was abolished when the antibodies were first preadsorbed with $HD_{549-679}$-GST (Fig. 1).

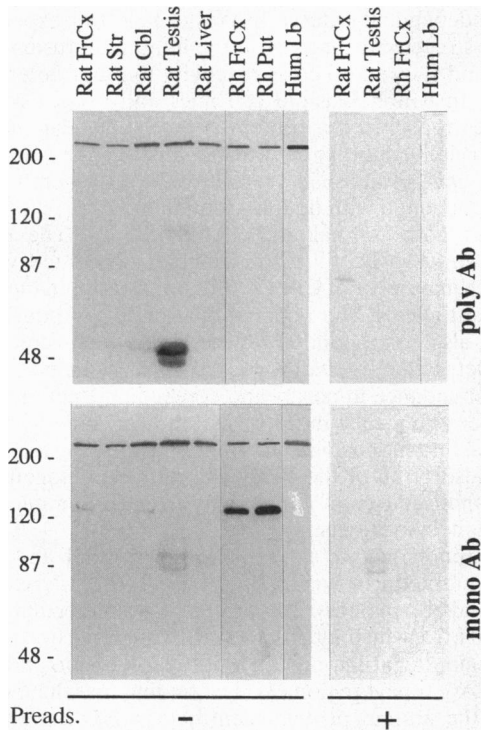

FIG. 1. Specificity of anti-huntingtin antibodies. Aliquots (50 μg of total protein) of rat, monkey, and human tissues were subjected to SDS/7.5% PAGE and immunoblotted with polyclonal (poly Ab) and monoclonal (mono Ab) anti-huntingtin antibodies. Molecular mass standards (in kDa) are indicated on the left. Rh, rhesus monkey; FrCx, frontal cortex; Str, striatum; Cbl, cerebellum; Put, putamen; Hum Lb, normal human lymphoblasts. In some cases the antibodies were preadsorbed (Preads.) with $HD_{549-679}$-GST fusion protein.

Western blotting was performed on lysates prepared from lymphoblast cell lines derived from heterozygote HD patients with various numbers of CAG repeats in the mutant alleles. In each lysate, immunoblotting revealed a doublet (Fig. 2) consisting of a lower band comigrating with the single band found in the samples from normal subjects and a higher molecular weight band of variable size corresponding to the mutant protein. The higher the number of CAG repeats in the mutant alleles, the slower the mobility of the upper protein (Fig. 2). In two cell lines derived from homozygote HD patients, only one band was detected on the immunoblots since both alleles had similar numbers of CAG repeats (one shown in Fig. 2). The molecular weight of this band was higher than that detected from normal alleles in control or heterozygote patients. Quantification of each band in the doublets from three HD juvenile patients was performed by optical densitometry, allowing comparison of the normal and mutant proteins within individuals. In the patient whose mutant allele contained more than 85 CAG repeats, mutant huntingtin level was only 30% of normal protein level (Fig. 2). In two other patients, with CAG repeats of 66 and 74, mutant huntingtin levels were 74% and 86% of normal protein levels, respectively (Fig. 2). These findings suggest that higher numbers of CAG repeats lead to lower levels of mutant than normal protein.

Light Microscopic Immunocytochemistry. The pattern of huntingtin expression as determined by immunocytochemistry was identical with both the polyclonal and monoclonal antibodies. Patterns of immunoreactivity in rat (data not shown), monkey, and human were very similar. Huntingtin appears to be highly expressed in the largest neurons in the brain, such as cortical pyramidal cells (Figs. 3 *a* and *b* and 4*a*), pallidal neurons (Figs. 3*e* and 4*d*), and Purkinje cells (Fig. 3*f*). Smaller neurons, such as interneurons in the cerebral and cerebellar cortices, were lightly stained (Fig. 3 *b* and *f*), as were some glial cells. In neurons, immunoreactivity filled perikarya and dendrites but was not seen within nuclei. Smaller caliber elements, such as dendritic spines and axons, were difficult to resolve, although occasional proximal axon segments of cortical pyramidal cells could be identified. In the monkey, caudate and putamen staining was homogeneous (Fig. 3*c*), with dense immunoreactivity in giant striatal interneurons and moderate staining in medium-sized cells (Fig. 3*d*). Striatal staining was more heterogeneous in the human (Fig. 4*c*), where increased staining in patch or striosome-like regions was evident (Fig. 4*b*).

EM Immunocytochemistry. The subcellular localization of huntingtin immunoreactivity when using DAB or immunogold

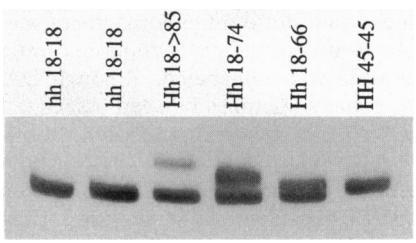

FIG. 2. Identification of normal and mutant forms of huntingtin. Aliquots (25 μg of total protein) of lysates prepared from lymphoblasts derived from control patients (hh), heterozygote HD patients (Hh), or a homozygote patient (HH) were subjected to SDS/4% PAGE and immunoblotted with monoclonal anti-huntingtin antibodies. One band is detected in cell lines derived from control and HD homozygote patients, whereas a doublet can be seen in cell lines derived from HD heterozygote patients. CAG repeat numbers for normal and mutant alleles were assessed as described elsewhere (3) and are indicated for each cell line.

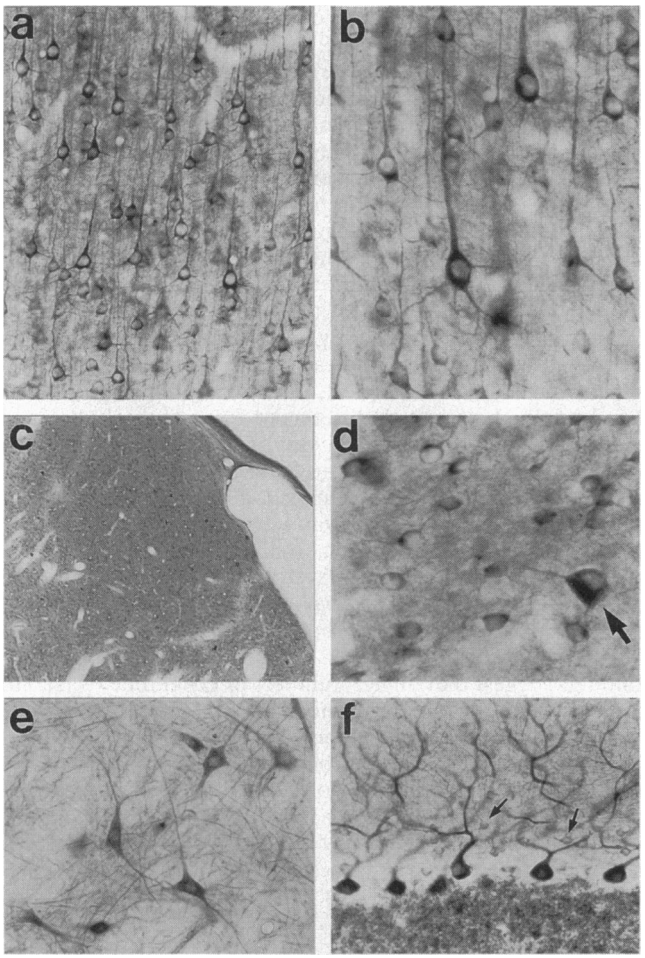

FIG. 3. Huntingtin immunocytochemistry in the monkey. Dense cellular staining is seen in the cerebral cortex (*a* and *b*), particularly in pyramidal cells and their dendrites. Staining is uniform in the caudate at low magnification (*c*). At higher magnification, giant interneurons (arrow) and medium-sized neurons are readily identified (*d*). Pallidal neurons and their dendrites are well stained (*e*). In the cerebellum, Purkinje cells have the highest intensity of staining, granule cells are moderately stained, and interneurons in the molecular layer (arrows) are barely discernible (*f*). (*a*, ×120; *b*, ×230; *c*, ×23; *d*, ×250; *e*, ×110; and *f*, ×110.)

was similar in cerebral cortex, putamen, and cerebellum. Most neuronal perikarya but few glia contained reaction product (Fig. 5*a*). Neither label was visualized within nuclei. Within perikarya, reaction product was cytosolic amid regions rich in free ribosomes, while little immunoreactivity was associated with Golgi apparatus or rough endoplasmic reticulum (Fig. 5*b*). Mitochondria were unlabeled, although DAB, but not immunogold, could sometimes be seen associated with their outer surfaces. Within dendrites, most DAB or immunogold particles were cytosolic and appeared to associate with microtubules (Fig. 5 *c–e*). Some labeling of endoplasmic reticulum and vesicles was also evident within dendrites. Despite intense dendritic immunoreactivity, only a small percentage of dendritic spines were labeled in each area examined (Fig. 5 *f* and *g*). Within labeled spines, there was some association between DAB and cell membranes and sometimes with postsynaptic densities (Fig. 5*f*). With immunogold labeling, however, associations with membranes or postsynaptic densities were rare. Most axons and axon terminals in cerebral cortex, striatum, and cerebellum were unlabeled. Those that were labeled contained reaction product associated primarily with synaptic vesicles (Fig. 5 *h* and *i*).

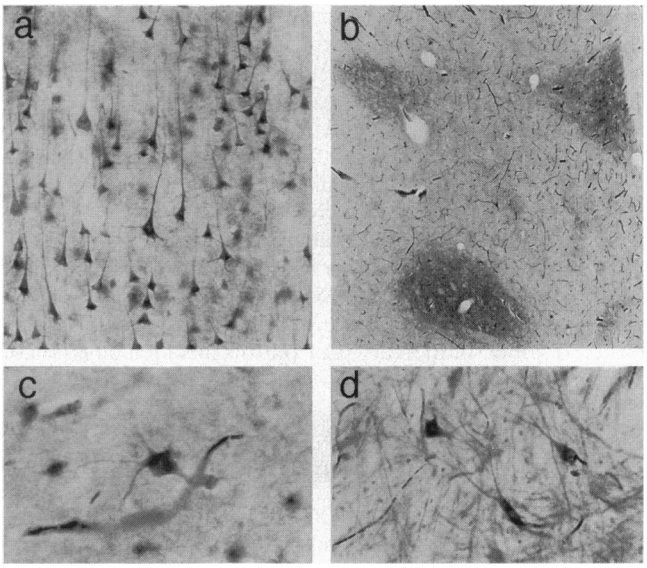

FIG. 4. Huntingtin immunocytochemistry in normal human. Cellular staining in the cerebral cortex (*a*), striatum (*c*), and pallidum (*d*) is similar to that observed in the monkey. However, in the caudate (*b*) and putamen (not shown), there is dense patchy labeling of the neuropil not seen in the monkey. Since the human tissue was not perfused, there is background peroxidase staining of blood vessels. (*a*, ×115; *b*, ×23; *c*, ×200; and *d*, ×100.)

DISCUSSION

In this study, we developed polyclonal and monoclonal antibodies for Western blotting and immunocytochemical localization of huntingtin in rat, monkey, and human tissues. The specificity and sensitivity of our antibodies were established by several independent criteria. In Western blotting experiments, antibodies reacted strongly with the huntingtin fusion protein antigen and showed no cross-reactivity to other heterologous proteins. In lymphoblastoid cell lines and brain tissues, the antibodies recognized a protein of the molecular mass predicted for native huntingtin. Most compelling, in lymphoblastoid cell lines established from juvenile HD heterozygotes, antibodies reacted with doublet protein bands detecting products from both normal and mutant alleles. The distance between the two bands of the doublet correlated with the difference in number of CAG repeat units between the normal and mutant alleles. The regional distribution of huntingtin in rat brain also corresponded well with the expression of *IT15* mRNA detected by *in situ* hybridization (7, 8), including higher protein abundance in cortex and cerebellum than in striatum and higher abundance in testis than in liver. Finally, both the polyclonal and monoclonal antibodies yield identical findings, and preadsorption of the antibodies with homologous fusion protein abolished immunoreactivity in both immunoblotting and immunocytochemistry.

In immunoblots, we have identified normal and mutant human huntingtin in lymphoblastoid cell lines derived from control and HD patients. The protein has a molecular mass of about 340 kDa, which is consistent with the large open reading frame beginning at the predicted initiation codon and including the CAG repeat region (3). The finding that the molecular mass of the mutant protein identified in HD heterozygotes increased as the CAG repeat number increased confirms that the repeat expansion is translated. Due to the high molecular mass of huntingtin, separation of both normal and mutant forms of huntingtin required a difference of at least 35 trinucleotide repeats between the normal and mutant alleles to be detected.

Immunoblot quantification performed on three HD lymphoblast cell lines indicated that the levels of the mutant form

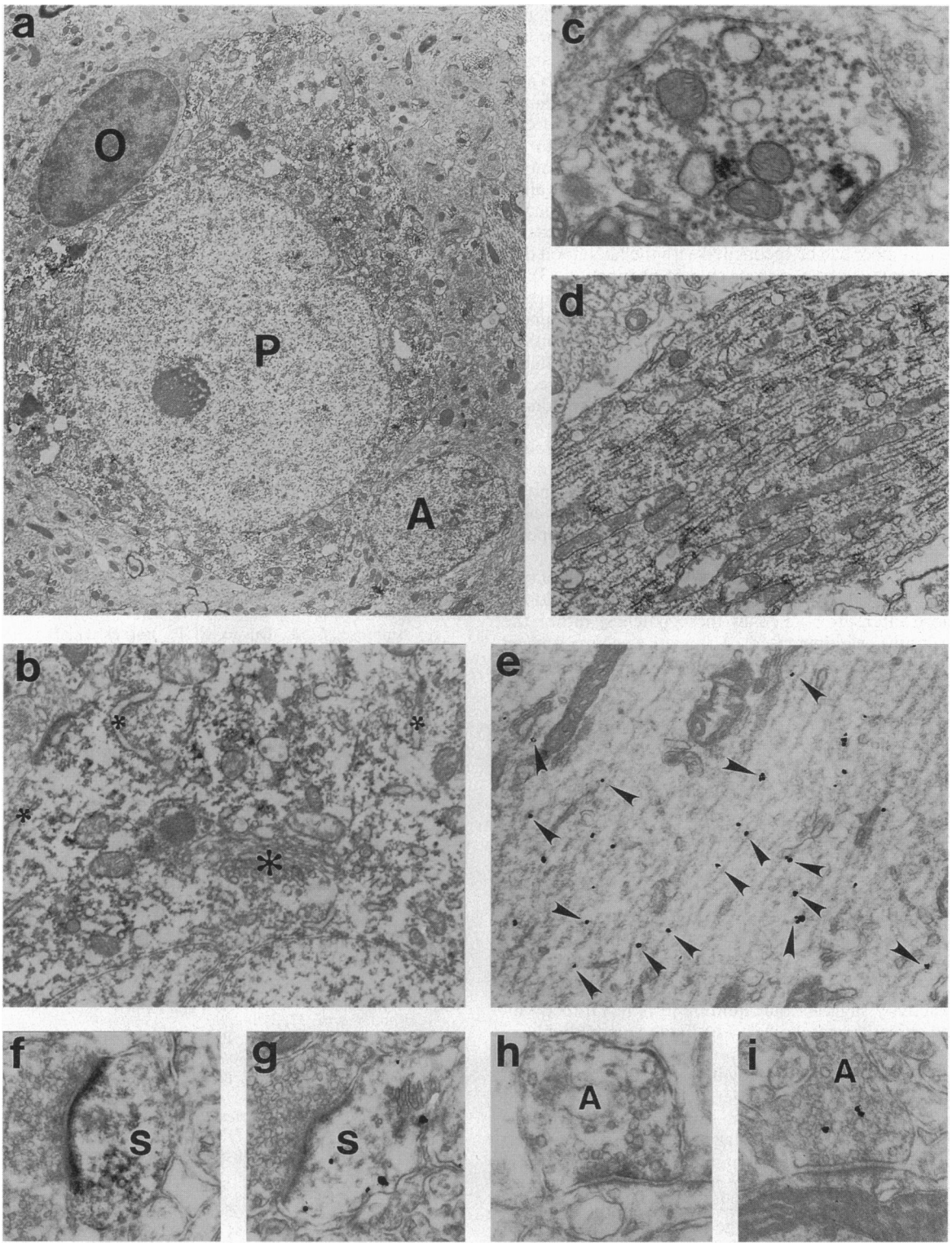

FIG. 5. Huntingtin EM immunocytochemistry in monkey. DAB reaction product is visible in a cerebral cortical pyramidal cell but not in an adjacent astrocyte or oligodendrocyte (*a*). Little of the cytoplasmic label in this cortical pyramidal cell is associated with Golgi apparatus (large asterisk) or rough endoplasmic reticulum (small asterisks) (*b*). A putaminal dendrite in cross section (*c*) and a Purkinje cell dendrite in longitudinal section (*d*) demonstrate that reaction product is either free in the cytoplasm or associated with microtubules. Immunogold labeling of a Purkinje cell dendrite, in longitudinal section, showing that many of the gold particles (arrowheads) contact microtubules (*e*). Dendritic spines (S) in the putamen (*f*) and cerebral cortex (*g*) are labeled with DAB and immunogold, respectively. Rare axon terminals (A) in the cerebellum (*h*) and cerebral cortex (*i*) contain DAB and gold particles, respectively. (*a*, ×4500; *b*, ×12,900; *c*, ×24,400; *d*, ×10,900; *e*, ×24,800; *f*, ×29,300; *g*, ×29,300; *h*, ×37,600; and *i*, ×43,500.)

of huntingtin is decreased relative to that of the normal form with a greater reduction occurring with larger repeat expansion. These reduced levels of mutant protein could reflect diminished protein synthesis due to a lower rate of mRNA transcription, a shorter mRNA lifetime, or a lower rate of mRNA translation. Alternatively, reduced mutant protein levels could be due to posttranslational effects, such as increased turnover, altered protein processing, or greater sus-

ceptibility to protease degradation. Since we did not detect lower molecular weight bands that might correspond to breakdown products, it is unlikely that the mutant protein in lymphoblasts is less stable under our assay conditions. It is also unlikely that CAG expansion causes conformational changes in the epitopes recognized by the antibodies and affects antibody binding since we used reducing and denaturing conditions in all our experiments. This reduction in mutant huntingtin must be confirmed in additional patients, as well as in brain and other tissues. If confirmed, it will be interesting to learn how decreasing levels of mutant protein with increasing CAG repeat number can be reconciled with the likelihood that the HD mutation causes a gain or change of function (3).

Huntingtin localization by immunocytochemistry is consistent with previous studies showing that most neurons appear to contain huntingtin mRNA, while glia contain little huntingtin mRNA (3, 7, 15). Larger neurons, which contain higher levels of mRNA (15), were the most immunoreactive for huntingtin. There were exceptions, however. Some medium-size cerebral and cerebellar cortical interneurons barely stained while medium-sized striatal cells and smaller cerebellar granule cells stained well. Huntingtin is abundant in perikarya and dendrites of cortical pyramidal cells and in Purkinje cells, which degenerate in HD (16, 17). However, large striatal interneurons, which were also highly immunoreactive for huntingtin, are preserved in HD (18).

A striking finding seen in human striatum was the patchy distribution of huntingtin expression. Striatal neurons did not appear more intensely stained in these patches, rather the neuropil staining was increased. Although we have not yet confirmed this observation with other labels, the huntingtin patches appear similar to striatal patches or striosomes (19). The increased expression of huntingtin within patches in human striatum may be related to the selective vulnerability of striatal neurons in HD. Although some studies indicate that striatal degeneration in HD may start in patches (20), this localization has not been found by other investigators (18).

Analysis of the subcellular localization of huntingtin provides some clues to its potential function. First, it is informative to consider which subcellular compartments do not contain huntingtin immunoreactivity. The lack of huntingtin in nuclei indicates that, unlike several other proteins with CAG repeats (21, 22), it is not a DNA-binding protein. The lack of immunoreactivity within rough endoplasmic reticulum and Golgi apparatus, suggests that huntingtin is not processed for export or insertion into membranes. The absence of mitochondrial immunoreactivity suggests that huntingtin is not directly involved with oxidative metabolism. The limited amount of label in dendritic spines or at presynaptic densities suggests that huntingtin is unlikely to be directly involved in synaptic transmission. Immunoreactivity, however, was most highly related to microtubules. We hypothesize that huntingtin may be involved in the primary microtubular functions of anchoring or transporting other molecules or organelles. Perhaps the HD mutation alters the anchoring or intracellular transport of mitochondria, RNA, or metabolically relevant proteins. Such an alteration could lead to an energetic defect and subsequent excitotoxicity, thereby providing a link between the genetic mutation and current ideas (1, 2) about neuronal death in HD.

We thank Dr. Randy Jones for her help in collecting blood samples and clinical data and Dwaine Blackstone for identifying one of the juvenile cases. We thank Drs. John Shoffner and Allan Kaufman for assaying CAG repeat length. We also thank Dr. David Rye for providing monkey and human tissue for immunocytochemistry. This work was supported by the U.S. Public Health Service (NS01624 and DA05002), the Hereditary Disease Foundation, the Emory University Research Committee, the American Parkinson's Disease Association, and the General Clinical Research Center (MO1-RR00039).

1. Beal, M. (1992) *Ann. Neurol.* **31,** 119–130.
2. Albin, R. & Greenamyre, J. (1992) *Neurology* **42,** 733–738.
3. Huntington's Disease Collaborative Group (1993) *Cell* **72,** 971–983.
4. Kremer, B., Golberg, P., Andrew, S. E., Theilmann, J., Telenius, H. C., Zeisler, J., Squitieri, F., Lin, B., Bassett, A., Almqvist, E., Bird, T. D. & Hayden, M. R. (1994) *N. Engl. J. Med.* **330,** 1401–1406.
5. Telenius, H., Kremer, B., Golberg, P., Theilman, J., Andrew, S. E., Zeisler, J., Adam, S., Greenberg, C., Ives, E. J., Clarke, L. A. & Hayden, M. R. (1994) *Nat. Genet.* **6,** 409–414.
6. Andrew, S. E., Golberg, Y. P., Kremer, B., Telenius, H., Theilmann, J., Adam, S., Starr, A., Squitieri, F., Lin, B., Kalchman, M. A., Graham, R. K. & Hayden, M. R. (1993) *Nat. Genet.* **4,** 398–403.
7. Li, A.-H., Schilling, G., Young, S. W., III, Li, X.-J., Margolis, R. L., Stine, O. C., Wagster, M. V., Abbott, M. H., Franz, M. L., Ranen, N. G., Folstein, S. E., Hedreen, J. C. & Ross, C. A. (1993) *Neuron* **11,** 985–993.
8. Strong, T., Tagle, D., Valdes, J., Elmer, L., Boehm, K., Swaroop, M., Kaatz, K., Collins, F. & Albin, R. (1993) *Nat. Genet.* **5,** 259–263.
9. Ambrose, C. M., Duyao, M. P., Barnes, G., Bates, G. P., Lin, C. S., Srinidhi, J., Baxendale, S., Hummerich, H., Lehrach, H., Altherr, M., Wasmuth, J., Buckler, A., Church, D., Housman, D., Berks, M., Micklem, G., Durbin, R., Dodge, A., Read, A., Gusella, J. & MacDonald, M. E. (1994) *Somatic Cell Mol. Genet.* **20,** 27–38.
10. Levey, A. I., Kitt, C., Simonds, W., Price, D. & Brann, M. (1991) *J. Neurosci.* **11,** 3218–3226.
11. Levey, A. I., Edmunds, S. M., Hersch, S. M., Wiley, R. G. & Heilman, C. J. (1995) *J. Comp. Neurol.* **351,** 339–356.
12. Blackstone, C., Moss, S., Martin, L., Levey, A. I. & Price, D. (1992) *J. Neurochem.* **58,** 1118–1126.
13. Hersch, S. M., Gutekunst, C.-A., Rees, H., Heilman, C. J. & Levey, A. I. (1994) *J. Neurosci.* **14,** 3351–3363.
14. Burry, R. W., Vandré, D. D. & Hayes, D. M. (1992) *J. Histochem. Cytochem.* **40,** 1849–1856.
15. Landwehrmeyer, G., McNeil, S., Dure, L., Ge, P., Aizawa, H., Huang, Q., Ambrose, C., Duyao, M., Bird, E., Bonilla, E., Young, M. d., Avilla-Gonzales, A., Wexler, N., DiFiglia, M., Gusella, J., MacDonald, M., Penney, J., Young, A. & Vonsattel, J.-P. (1995) *Ann. Neurol.* **37,** 218–230.
16. Sotrel, A., Paskevich, P., Kiely, D., Bird, E., Williams, R. & Myers, R. (1991) *Neurology* **41,** 1117–1123.
17. Jeste, D. V., Barban, L. & Parisi, J. (1984) *Exp. Neurol.* **85,** 78–86.
18. Ferrante, R., Kowall, N., Beal, M., Richardson, E., Bird, E. & Martin, J. (1985) *Science* **230,** 561–563.
19. Gerfen, C. R. (1992) *Trends NeuroSci.* **15,** 133–139.
20. Hedreen, J. & Folstein, S. (1995) *J. Neuropathol. Exp. Neurol.* **54,** 105–120.
21. Perutz, M., Johnson, T., Suzuki, M. & Finch, J. (1994) *Proc. Natl. Acad. Sci. USA* **91,** 5355–5358.
22. Mhatre, A., Trifiro, M., Kaufman, M., Kazemi-Esfarjani, P., Figlewicz, D., Rouleau, G. & Pinsky, L. (1993) *Nat. Genet.* **5,** 185–188.